Elastic material properties of sand piles of soft convex polygonal particles

Pradip Roul [1,*], Alexander Schinner[2], Klaus Kassner[1]

[1] Institute of Theoretical Physics, Otto-von-Guericke University Magdeburg, Postfach 4120, D-39106 Magdeburg, Germany

[2] T-Systems, Dachauer Straße 665, 80995 München

Abstract We investigate the effective material properties of sand piles of soft convex polygonal particles numerically using the discrete element method (DEM). We first construct two types of sand piles by two different procedures. We then measure averaged stress and strain, thelatter via imposing a 10% reduction of gravity, as well as the fabric tensor. Furthermore, we compare the vertical normal strain tensor between sand piles qualitatively and show how the construction history of the piles affects their strain distribution as well as the stress distribution. In the next step, we determine the elastic constants, assuming Hooke's law throughout the sand piles, and the correlation between the elastic material conefficients and the fabric tensor. We observe that the bulk modulus of the sand pile, i.e., the stiffness of the granulate is a linear function of the trace of the fabric tensor. We determine the relationship between invariants of the stress and strain tensor, observing that the behaviour is nonlinear which means that we have linear elastic behavior near the centre of the pile and nonlinear behavior announcing the transition to plastic behavior near the surface of the sand piles, the same behavior as was assumed by Cantelaube et al. [1]. We find that the macroscopic stress and fabric tensors are not collinear in the sand pile.

1 Introduction

In the last few years, extensive research has been devoted to the study of granular materials due to their importance for applications in various industries and because they pose fundamental analytical challenges [1],[2]. An important question is to understand the mechanical properties of non-cohesive granular matter, especially in the static limit. In this regard, the simplest example out of a collection of granular arrangements is the static sand pile, and the practice of storing granular materials in the form of sand piles occurs in many industrial situations. In order to handle the processing of granular materials in a sand pile properly, it is important to understand its mechanical properties and effective material behavior.

The stress distribution under a pile of sand displays some puzzling properties. Depending on characteristics such as the size and shape distribution of particles but also the construction history of the aggregate, two piles consisting of the same material may have different stress distributions [3]. If the material is dropped from a point source, there is a stress minimum, if it is dropped layer-wise, there is no minimum. However, in some cases, the stress distribution displays a pronounced minimum below the tip of the sand pile and in others it has a small minimum [4]. If the sand pile contains a mixture of ellipsoidal particles, there is a large stress dip below the tip of the pile for a certain construction history of the pile, whereas when it contains a mixture of roundish particles, there is a much smaller dip.

To a certain extent, even more interesting than studying the stress tensor is to determine the strain distribution under a sand pile. One might regard it as one of the essential questions in the field of granular heaps, how deformation under stress can be defined, aiming at the identification of a strain tensor and establishing a correlation between the stress and strain tensors in order to determine effective material properties. Up to now, no strains have been measured in experiments on sand piles. Theoretical models and analysis assume that for sand piles displacement fields are not available. Therefore, constitutive relations proposed for sand piles [1],[2] have been obtained without introduction of a strain tensor.

In this paper, we focus on the sensitivity of the strain distribution to the preparation of sand piles. The main aim of this study is to investigate numerically the effective material properties of sand piles. By performing

a discrete element method (DEM) simulation, we obtain a macroscopic strain tensor from microscopic quantities such as displacements of the individual grains in a two-dimensional sand pile. Then we can estimate local elastic constants assuming Hooke's law. Generally speaking, if we find almost constant values of elastic constants throughout the sand piles, linear elasticity may be considered a good approximation. If we get, on the other hand, strongly varying elastic constants, then we can say that linear elasticity is not going to work for the pile as a whole. Moreover, this computation serves as a consistency check for theoretical assumptions such as the rigid-particle hypothesis. If our calculation produced elastic constants of the same order of magnitude as the Young's modulus that we assign to the particles to allow an overlap for force calculation, then the idea that the sand pile has a macroscopic elastic behavior different from that of its microscopic constituents would not be valid because the elastic constants of the pile would go to infinity with those of the grains. This idea can work only, if the sand pile admits a finite elastic response in spite of the rigidity of the grains, which means that the elastic coefficients of the sand pile must be significantly smaller in the simulation than those of the particles.

The paper is organized as follows. In Section 2, we first describe our discrete element method (DEM) simulation of two dimensional sand piles consisting of soft convex polygonal particles. In Section 3, we determine the stress tensor as well as the strain tensor, adopting Cambou's best fit strain approach for the latter. We discuss the averaging procedure used to extrapolate to macroscopic fields. Then we present simulation results for averaged vertical normal strains at different heights inside a sand pile poured from either a point source or a line source. We give a formula for the fabric tensor of polygonal particles and discuss its different properties in Section 4. Once we have the stress and strain tensors, we determine the elastic constants assuming Hooke's law. Then, we measure effective material properties of the sand piles that are poured from a point source and establish a correlation between elastic constants and fabric tensor, discussed in Section 5. We also determine the relation between the stress and strain tensors in Section 6. At last, we give some conclusions from our results in Section 7.

2 Simulation method

We perform numerical simulations, in which a sand pile is constructed from several thousand convex polygonal particles with varying shapes, sizes and edge numbers. The particles are poured from either a point source, which regularly leads to a pressure minimum under the pile, or a line source. We use a discrete-element method with soft but shape-invariant particles: two particles in contact with each other are allowed to interpenetrate partially. On the one hand, it would be inefficient to solve the elastic equations for each collision between pairs of nonrigid particles, on the other, to implement an event-driven code allowing the (desirable) solution of the equations of motion for rigid particles would be too cumbersome with polygonal particles.

We solve the equations of motion following from the balances of momentum and angular momentum for each particle, using a fifth-order Gear predictor-corrector method [5]. Colliding particles overlap. Forces are then calculated from the geometric characteristics overlap area and contact length (defined as the distance between the two points of intersection of the overlapping polygons) using the relative velocities of the two particles. The calculation involves phenomenological elastic constants as well as model parameters for friction and viscous damping. Details are given in [6].

In two dimensions, the momentum balance provides two equations per particle, the angular momentum balance one:

$$m_i \ddot{\mathbf{r}}_i = \sum_{j=1}^{n} \mathbf{F}_{ij} + \mathbf{G}_i \,, \qquad I_i \ddot{\varphi} = \sum_{j=1}^{n} L_{ij} \,. \tag{1}$$

Here, the subscript *i* runs over all the particles, the subscript *j* over all the contacts of particle *i* with other particles. That is, forces and torques are exchanged between particles only if they touch. Hence we have short-range forces, viz. contact forces. $\mathbf{G}_i$ is the force acting on particle *i* due to external fields, in our case

just gravitation, $\mathbf{F}_{ij}$ the force created by the particle touching particle *i* in contact *j*. There is at most one contact between two particles as our polygons are restricted to being convex.

The force calculation is one of the most time-consuming parts of the algorithm. Of course, advantage is taken of the short-range nature of the forces by calculating only non-vanishing forces, i.e., forces between particles that are really in contact with each other. To achieve fast contact determination in a time that is proportional to the number of particles (not to its square), independent of the complexity, i.e., the number of edges of the particles, algorithms from virtual reality and computational geometry were adapted. These use bounding boxes and Voronoi regions to determine overlaps of particles [6].

We solve Newton's and Euler's equations of motion involving the forces and the torques acting on each particle, using a fifth-order Gear predictor-corrector method. Magnitude, direction and point of application of the microscopic force between two colliding particles are calculated from the area and contact length of their overlap.

3. Stress calculation

Once we have the forces, we can compute stresses. It is easy to derive a formula for the average stress obtained in a homogeneous polygonal particle [7], assuming that the forces given in the contact points act on the corresponding edge of the polygon:

$$\sigma_{ij}^{p} = \frac{1}{V^{p}} \sum_{c=1}^{m} x_i^c f_j^c , \qquad (2)$$

where x_i^c is *i*-th component of the branch vector pointing from the center of mass of the particle to the contact point *c*, and f_j^c is the *j*-th component of the total force in that contact point. V^p is the volume of particle *p* (actually an area, since we are in 2D) .

Expression (2) may be interpreted as the stress tensor associated with a single particle. This microscopic stress would not be a convenient means to describe the macroscopic sandpile, as it fluctuates wildly within a volume containing a few sand grains. Moreover, it is not defined in the voids between the grains. Hence, for a continuum description, we need to average microscopic stresses.

A representative volume element (RVE) is introduced via the requirement that the average becomes size independent, if the volume is taken equal to this value or larger. Averaging over different volumes gives different results, as long as the volume element is too small. As we increase the size of the volume element in the computation of the average, the latter converges to a certain value as shown in Fig.1. We find that sizes of the volume element containing 100-200 particles are sufficient to serve as RVE.

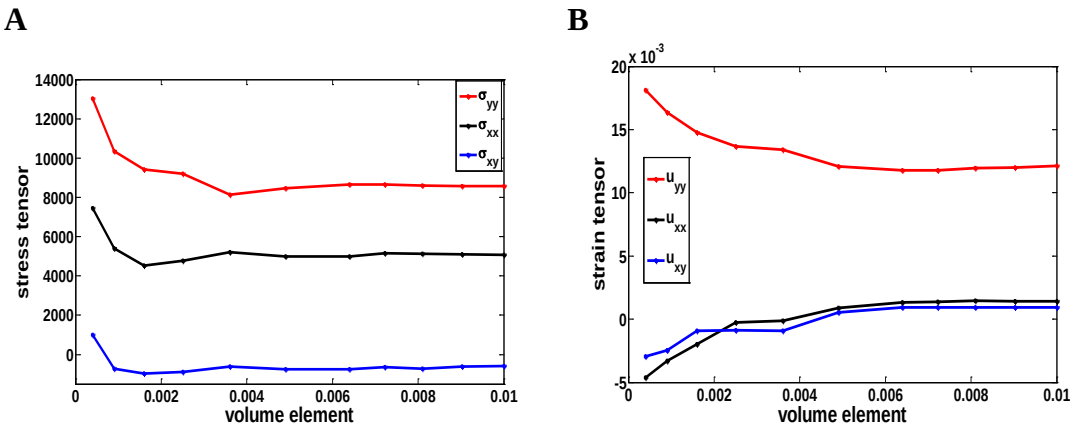

Fig.1: (A) Representative volume element (RVE) for stress tensor, and (B) RVE for strain tensor.

While the calculation of stresses is rather straightforward, this is not true for strains. In fact, even the definition of strain is problematic after assuming particles to be essentially rigid. For this reason, most macroscopic descriptions proposed in the last few years try to get by without using strain at all. Whether this approach can be successful in the long run remains to be seen. In any case, even if it may be difficult or impossible to determine strains in *experiments* on sand piles, this is not quite so in a *simulation*.

Our original idea was to define strains with respect to a hypothetical reference state of zero gravity of a sand pile essentially identical to the one at ambient gravity, except of course for slightly displaced particle centers. In this reference state, no particle rearrangements should be present in comparison with the actual state. The reference state would then be obtained from the ambient one by slowly reducing gravity. In principle, it is not necessary to go down to zero gravity, as long as the strains increase linearly with the gravity level – one may then extrapolate to zero from the knowledge of the positions of the particle centers of mass at two arbitrary different gravity levels. But it is necessary to let the sand pile approach a state of rest after a reduction of gravity. Moreover, linearity has to be checked by looking at different gravity levels.

This method does not work as expected, since a reduction of gravity leads to a proportional reduction only of normal stresses corresponding to the direction of gravity, i.e. σ_{yy}, but not σ_{xx}. Stresses in the *x* direction are essentially due to static friction of the pile with its support. Since most contacts are not fully mobilized, contact forces at the bottom of the pile are not strictly proportional to the normal force (their weight); the effective friction coefficient can vary between 0 and μ during a change of the gravity level. Hence, the method does not yield absolute displacements, as we have no access to the hypothetical reference state. Nevertheless, it is of course still possible to determine incremental strains, which are defined as the strain changes between the actual state and a state at a different gravity level. Using incremental stresses as well, we are then in a position to determine elastic coefficients.

We are aware of two ways given in the literature for determining averaged strains in an assembly of grains. First the equivalent continua theories (Bagi [8]; Satake [9]) and second the least-square fit theories (Cambou et al. [10]). In our study, we used one of the simplest techniques, namely the best-fit strains of Cambou et al. [10] who consider the relative translation instead of the contact deformations, which means to exclude particle rotations from the analysis. Displacements are characterized in terms of the translations of the particle centers.

Let du_j^p denote the translation of the centre of particle *p*.The relative translation of the pairs of grains *p* and *q* forming contact *c* is

$$d\Delta u_j^c = du_j^q - du_j^p \tag{1}$$

If every particle of assemblies of grain moved according to a uniform displacement gradient tensor ε_{ji}, then the relative translation at contact *c* would be

$$d\Delta u_i^c = \varepsilon_{ji} l_j^c \tag{2}$$

where l_j^c is the branch vector at the contact point.

However, usually this is not the case, and for a general case, we would have

$$d\Delta u_i^c \neq \varepsilon_{ji} l_j^c \tag{3}$$

Then, we determine the tensor ε_{ji} for which the square sum of the deviations in (3) is the smallest i.e, we minimize the following quantity

$$Z = \sum_c (d\Delta u_j^c - \varepsilon_{ji} l_j^c)^2. \tag{4}$$

with respect to ε_{kl}, i.e., we set $\frac{\partial Z}{\partial \varepsilon_{kl}} = 0$ for every *k,l*.

Equation (6) gives four equations in 2D which can be written in matrix form as follows

$$\begin{pmatrix} \sum_{c=1}^{n} l_1^c l_1^c & \sum_{c=1}^{n} l_2^c l_1^c \\ \sum_{c=1}^{n} l_1^c l_2^c & \sum_{c=1}^{n} l_2^c l_2^c \end{pmatrix} \begin{pmatrix} \varepsilon_{1i} \\ \varepsilon_{2i} \end{pmatrix} = \begin{pmatrix} \sum_{c=1}^{n} d\Delta u_i^c l_1^c \\ \sum_{c=1}^{n} d\Delta u_i^c l_2^c \end{pmatrix} \qquad (5)$$

(*i* is 1 or 2)

The coefficient matrix on the left-hand side of (5) is positive definite if there exist at least two branch vectors in the system that are not parallel to each other. This is the necessary and sufficient condition of the existence of the Cambou et al. best-fit strain in 2D.

Let z_{ij} denote the inverse of the coefficient matrix. In order to determine the ε_{11} and ε_{21} we substitute $i = 1$, whereas $i = 2$ is substituted for the calculation of ε_{12} and ε_{22}.

The solution of (5) can be written in the general form

$$\varepsilon_{ij} = z_{ik} \sum_c d\Delta u_j^c l_k^c \quad i, j, k = 1,2 \qquad \text{(summation over } k \text{ implied)} \qquad (6)$$

The tensor ε_{ij} in equation (6) is the best-fit translation gradient of Cambou et al. The components of the strain tensor in two dimensions are as follows

$$\varepsilon_{xx}(x,y) = \sum_c d\Delta u_x^c \left(z_{11} l_x^c + z_{12} l_x^c \right)$$
$$\varepsilon_{yy}(x,y) = \sum_c d\Delta u_y^c \left(z_{21} l_y^c + z_{22} l_y^c \right)$$
$$\varepsilon_{xy}(x,y) = \sum_c d\Delta u_y^c \left(z_{11} l_x^c + z_{12} l_y^c \right)$$
$$\varepsilon_{yx}(x,y) = \sum_c d\Delta u_x^c \left(z_{21} l_x^c + z_{22} l_y^c \right)$$

The box size we use for the computation of the strain tensor is the same as for the stress tensor.

Simulation results

The vertical normal strain tensor component obtained from DEM simulations is displayed in Fig.2. for two types of sand piles that were constructed using the two different pouring protocols. The averaged strain tensor was evaluated throughout the sand pile; typically, we represent it via a plot of tensor components as a function of the lateral coordinate *x* of the pile for layers of given heights $y_1, y_2, \ldots y_n$.

We give this component of the strain tensor to obtain a qualitative picture, although the foregoing discussion shows that it is not a rigorously determined quantity. While it has the correct scaling with gravity level, vertical and horizontal strains are of course coupled, so the errors produced by the method in the horizontal direction will also affect the vertical direction. The topmost curve in the graph shows the strain tensor result at the bottom layer of the corresponding sand pile, whereas the bottom curve corresponds to the top layer. An interesting feature of the vertical normal strain tensor for various heights is that the verti-

cal normal strain changes with the layer position in the sand piles like the stress tensor. The vertical normal strain shows a dip (Fig.2.A) near the centre of the piles that are poured from a point source. It can be seen that the strain dip appears not only at the bottom layer but also exists up to the certain height of the sand pile (Fig.2.B). The vertical normal strain increases towards the centre and towards the bottom layer of sand piles poured from a line source. A strain dip does not occur in the profiles of sand piles constructed from a line source.

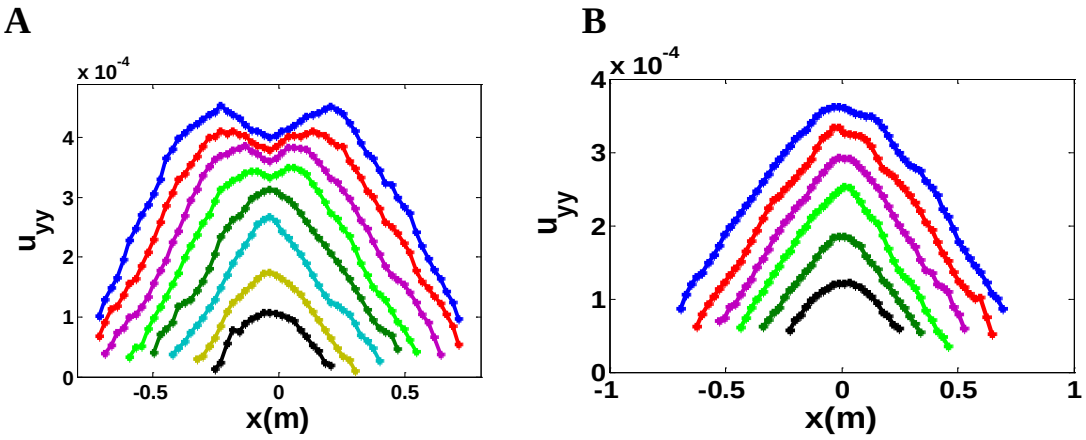

Fig.2: Vertical normal strain distribution at different heights of simulated sandpiles. Left: sand piles constructed from a point source (average over 9 piles), right: sand piles poured from a line source (average over 10 piles).

4. Fabric tensor

The density distribution is not homogeneous under a sand pile that is poured from a point source. Therefore, it may be said that the internal texture of the pile is important. Furthermore, forces are propagated from one particle to the neighbour particles in an assembly of grains only via at the contacts point of the particle. Thus, for the quasi-static mechanics of granular aggregates, it is necessary to describe the associated contact network of the inter-particle contacts.

A particular quantity that describes the internal texture of the granular assembly is the so-called fabric tensor [11],[12]. Various definitions of the fabric tensor exist in the literature including definitions for elliptical, spherical or polygonal particles. In our study, we consider non-spherical particles so we employ here a mathematical formulation for the fabric tensor, in which the branch vector itself is used to define a unit vector in the direction towards the contact, because here the simplest way of characterizing the packing network is via the branch vectors connecting the particle centres of mass with their contacts.

Once we have the contact points of the individual particles, we can calculate a fabric tensor for each particle, which yields an additive contribution to the overall fabric tensor. The latter then is a volume average over many particles. After defining the fabric tensor for one particle and for an aggregate of grains, we will demonstrate how it may be used to examine for isotropy of the granular structure of a material. The fabric tensor measures the contact number density in a given direction in the assembly. Therefore, it might be used to examine whether the grains of the material are placed in an isotropic way or whether there exists any directional ordering.

The fabric tensor for one particle

The general formula for the fabric tensor of single particle is given [11][12] by

$$F_{ij}^{p} = \sum_{c} n_i^c n_j^c \qquad (7)$$

Where n_i^c is the *i*th component of the unit normal vector at the contact point *c* of the considered particle *p*.

$$n_i^c = \frac{x_c - x_p}{\sqrt{(x_c - x_p)^2 + (y_c - y_p)^2}}$$

$$n_i^c = \frac{y_c - y_p}{\sqrt{(x_c - x_p)^2 + (y_c - y_p)^2}}$$

where (x_c, y_c) and (x_p, y_p) are the contact point and the center of mass, respectively, and the sum in (7) is over all the contacts of the particles.

The trace of the fabric tensor determines the number of contacts of particle *p*:

$$tr(F_{ij}^{p}) = \sum_{c} n_i^c n_j^c = C^p$$

We take an average over many particles in a representative volume element in order to determine the average fabric tensor that describes the contact network in a given volume *V*.

Properties of the fabric tensor

The fabric tensor is symmetric by definition and therefore normally consists of three independent components in two dimensions. These may be expressed in a largely coordinate independent way using tensor invariants and geometrical quantities.

As the first of these quantities, we choose the trace of the fabric tensor, which is a scalar. It is also known as the volumetric part of the fabric and given by $tr(F) = F_{\max} + F_{\min}$, where $F_{\max}$ and $F_{\min}$ are the major and minor eigenvalues of the fabric tensor, respectively. In Fig.3A, the trace of the averaged fabric tensor is plotted at different heights inside the sand pile. It can be seen from the figure that the mean number of contacts decreases near the surface of the sand pile and increases with increasing distance from the surface to the centre of the sand pile. Since we have measured the density to increase towards the centre of the pile in the case of a pile poured from a point source, this means that the number of contacts is higher where the density is maximum.

As a second independent quantity determining the fabric tensor we may choose the fabric deviator. It is defined as $F_D = F_{\max} - F_{\min}$ and is a measure of the degree of anisotropy in the contact network of the granular assembly. The deviatoric fraction of the fabric tensor $F_D / tr(F)$ is plotted in Fig 3.B for different heights inside the sand pile. From the figure, it is observed that the deviatoric fraction decreases towards the centre. This means that the fabric is more isotropic near the centre of the sand pile and more anisotropic in the outer part. The fabric anisotropy is between 0.05 and 0.15.

The angle of the orientation of the major eigenvector of fabric tensor may serve as the third independent quantity defining the fabric tensor. The orientatation of the major eigenvector with respect to the horizontal axis is given in Fig 3.C at different heights inside the sand pile. It changes from -40 degrees (left) to +40 degrees (right).

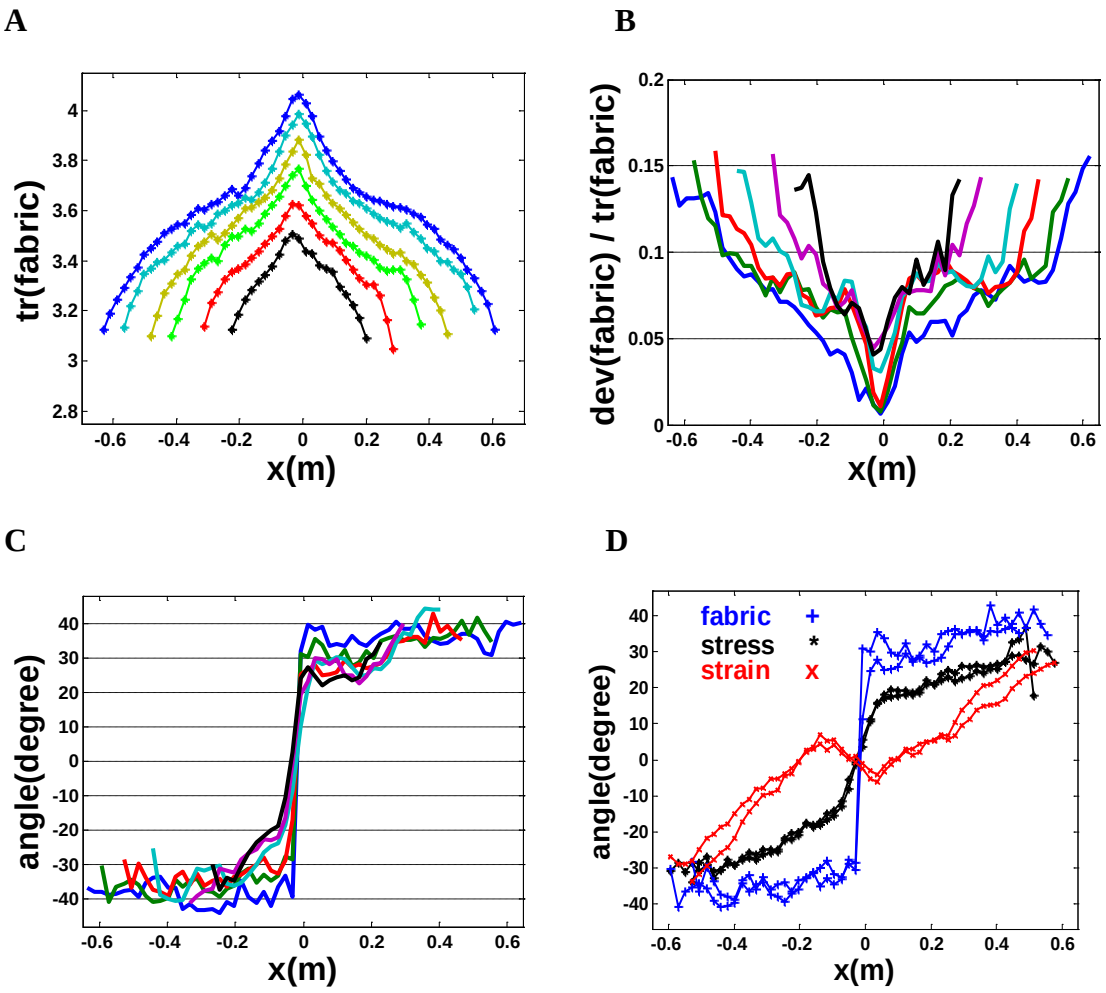

Fig.3 A-D. (A) trace of the fabric tensor, (B) deviatoric fraction, (C) orientation of fabric versus lateral position in the sand pile, and (D) orientation of fabric, stress and strain plotted only for the first two bottom layers of the pile.

The orientation of three macroscopic tensors stress, strain and fabric are plotted in Fig. 2.D only for the first two bottom layers of the pile. No meaning should be attributed to the deviation of the strain tensor from the behavior of the stress tensor, since the *xx* and *xy* components of the former cannot be determined reliably. It can be seen, however, that the orientations are different also for the fabric and stress tensors, which means that these macroscopic tensors are not collinear. Most likely this limits the utility of a description of granular piles in terms of isotropic elasticity. Nevertheless, we shall consider such a description in the following to explore these limitations in some detail.

5. Determination of elastic constants

Once we have the stress tensor and strain tensor we can determine the effective material properties of sand piles assuming Hooke's law. Under the assumption that the material is locally isotropic, we can characterize its elastic constants using only two coefficients, for example Young's modulus and Poisson's ratio. The relation between stress tensor and strain tensor reads

$$\sigma_{ik} = \frac{E}{1+\nu}\left(u_{ik} + \frac{\nu}{1-2\nu} u_{ll}\delta_{ik} \right)$$

Written out in components for the two dimensional case this becomes

$$\sigma_{xx} = \frac{E}{(1+\nu)(1-2\nu)}((1-\nu)u_{xx} + \nu u_{yy}) \tag{8}$$

$$\sigma_{yy} = \frac{E}{(1+\nu)(1-2\nu)}((1-\nu)u_{yy} + \nu u_{xx}) \tag{9}$$

$$\sigma_{xy} = \frac{E}{(1+\nu)}u_{xy} \tag{10}$$

In our case, the unknown quantities are E and ν.

Equations (8) and (9) allow us to obtain simple expressions for the trace and the first normal stress difference

$$\sigma_{xx} + \sigma_{yy} = \frac{E}{(1+\nu)(1-2\nu)}(u_{xx} + u_{yy}) \tag{11}$$

$$\sigma_{xx} - \sigma_{yy} = \frac{E}{(1+\nu)}(u_{xx} - u_{yy}) \tag{12}$$

Next, we determine the best approximation for E and ν satisfying all three equations (10), (11), and (12) as closely as possible. This is a minimization problem for given fields σ_{ij} and u_{ij}, which may be cast as follows. Set

$$\begin{aligned} f(\nu,E) = {} & [(1+\nu)(1-2\nu)(\sigma_{xx}+\sigma_{yy}) - E(u_{xx}+u_{yy})]^2 \\ & + [(1+\nu)(\sigma_{xx}-\sigma_{yy}) - E(u_{xx}-u_{yy})]^2 + [(1+\nu)\sigma_{xy} - Eu_{xy}]^2 \end{aligned} \tag{13}$$

and minimize this expression with respect to E and ν. That is, we set

$$\frac{\partial f}{\partial E} = 0 \ , \quad \frac{\partial f}{\partial \nu} = 0$$

and these two equations should be solved for E and ν in principle. It is found that they constitute a nonlinear system that cannot be solved analytically (though a numerical solution should not be too difficult). A simpler approach is to use two different elastic constants, also well-known, namely the bulk modulus *K* and the shear modulus *G*, which are are related to Young's modulus and the Poisson number via the following equations:

$$K = \frac{E}{2(1+\nu)(1-2\nu)} \tag{14}$$

$$G = \frac{E}{2(1+\nu)} \tag{15}$$

which allows us to rewrite the above equations in terms of *G* and *K*, to obtain

$$\sigma_{xx} + \sigma_{yy} = 2K(u_{xx} + u_{yy})$$

$$\sigma_{xx} - \sigma_{yy} = 2G(u_{xx} - u_{yy})$$

$$\sigma_{xy} = 2Gu_{xy}$$

Then we minimize the expression

$$g(G,K) = [(\sigma_{xx}+\sigma_{yy}) - 2K(u_{xx}+u_{yy})]^2 + [(\sigma_{xx}-\sigma_{yy}) - 2G(u_{xx}-u_{yy})]^2 + 4[\sigma_{xy} - 2Gu_{xy}]^2 \tag{16}$$

with respect to *G* and *K*, i.e., we set

$$\frac{\partial g}{\partial G} = 0,\ \frac{\partial g}{\partial K} = 0 \tag{17}$$

Solving the simplified equations for K and G we obtain

$$K = 0.5 * \frac{\sigma_{xx} + \sigma_{yy}}{u_{xx} + u_{yy}} \tag{18}$$

$$G = 0.5 * \frac{(\sigma_{xx} - \sigma_{yy})(u_{xx} - u_{yy}) + 4\sigma_{xy}u_{xy}}{(u_{xx} - u_{yy})^2 + 4u_{xy}u_{xy}} \tag{19}$$

Note that this calculation works the same way with incremental stresses and strains, so we can determine elastic constants even though we cannot obtain the absolute strain tensor. Once K and G have been determined, we can calculate E and ν as follows,

$$\nu = 0.5\left(1 - \frac{G}{K}\right) \tag{20}$$

$$E = 3G - \frac{G^2}{K} \tag{21}$$

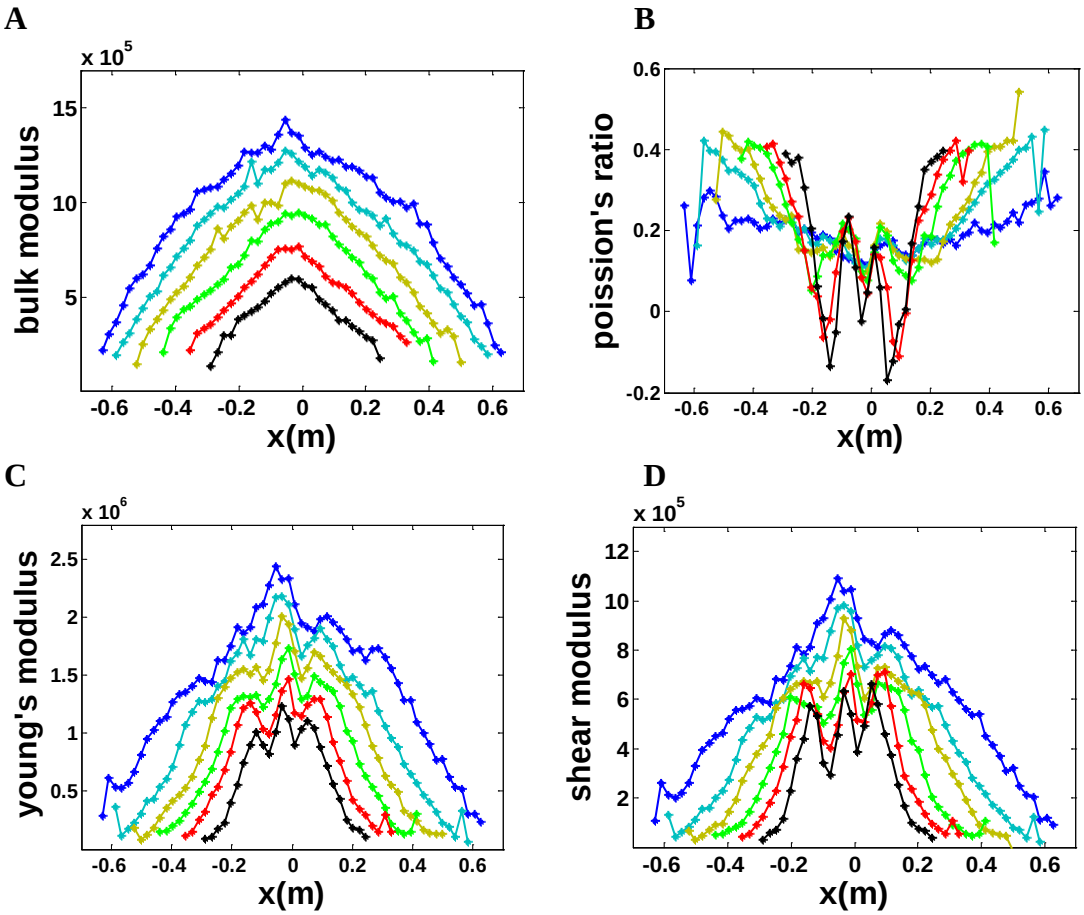

Fig.4- Effective material properties from simulation of sand pile poured from a point source.

The effective material properties as obtained in simulations of sand piles that were constructed from a point source are shown in Fig.4.A-D. We measured the elastic constants at different heights of the sand pile. The

topmost curve in panels A, C, and D corresponds to the results for the bottom layer, whereas the bottom curve was measured the top layer of the sand piles. For Fig. 4B, the layer to which a curve corresponds may be gathered from the domain of definition of the curve: this is largest for the bottom layer and smallest for the top layer (so the curve with the smallest variation corresponds to the bottom layer). We find that the elastic constants vary with position inside the sand pile. It may also be noted that the density changes as a function of the layer position in the sand pile, moreover, we observe that the middle region of the sand piles displays higher density than the rest (not shown). In addition, we see that the elastic constants Young's modulus of elasticity, shear modulus, and bulk modulus increase towards the centre and towards the bottom, and decrease towards the surface with very little fluctuation, but the correlation with the density is not really clear.

We use a Young's modulus of $E = 10^7 N/m$ for each particle and the scale of the measured elastic modulus of the sand pile is approximately $E = 10^6 N/m$, i.e. one order of magnitude smaller for small load as we reduced gravitation by only 10% .That means, the simulated sand pile is softer around one order of magnitude than its individual particles indicating the decrease in the stiffness of the sandpiles.The bulk modulus is observed to increase towards the centre as expected, indicating the central core region of the heap is much harder than the region closer to the surface. It can be seen in Fig 3D that Poisson's ratio behaves differently as it increases towards the surface of the sand pile and decreases towards centre and tip of the sand pile, especially, it fluctuates more near the tip of the sand pile.

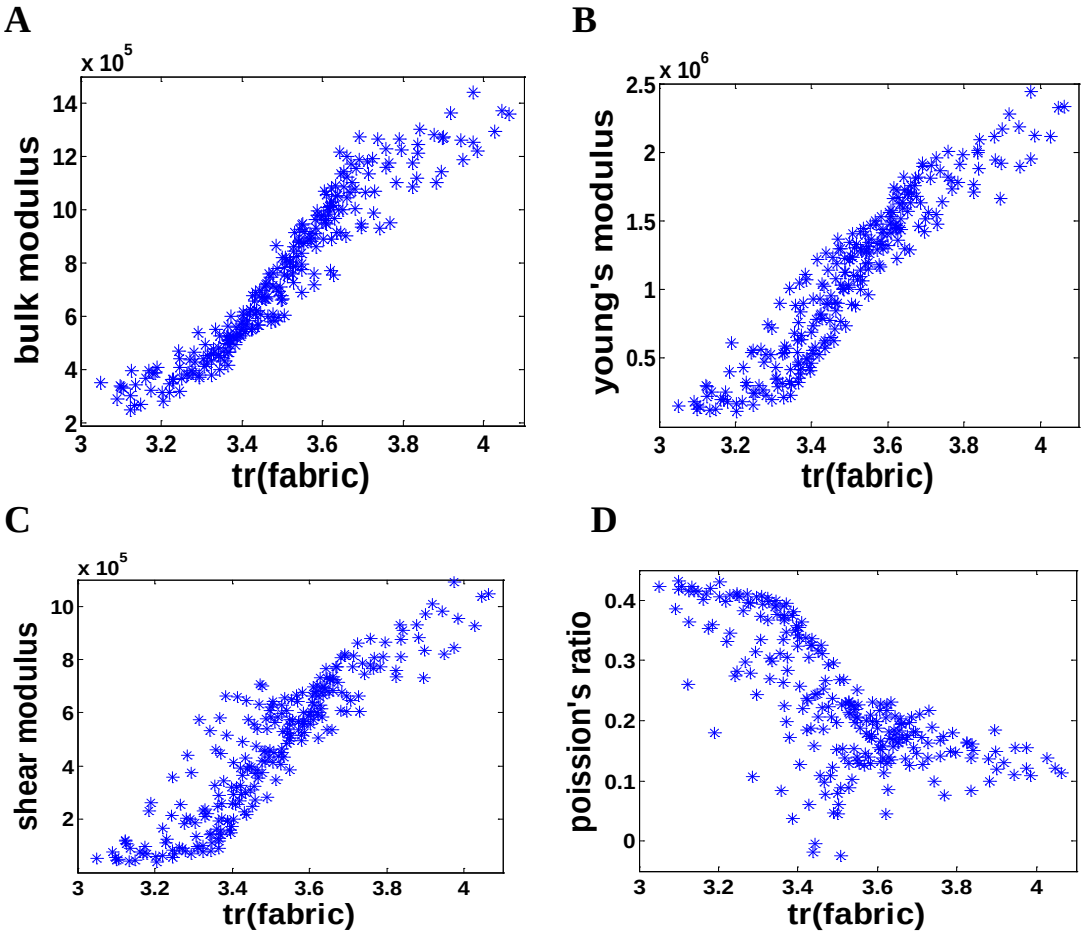

Fig.5- Correlation between elastic constants with the trace of the fabric tensor. (A) Bulk modulus of elasticity (B) Youngs's modulus of elasticity, (C) Shear modulus, and(D) Poisson's ratio, plotted against the trace of the fabric tensor throughout the sand pile.

In Fig. 5, we establish a correlation between elastic constants and trace of the fabric tensor. In Fig. 5A, we plot the bulk modulus of the macroscopic sand piles against the trace of fabric tensor. Obviously, the be-

haviour is linear to a decent approximation, i,e the stiffness of the particles is a linear function of the trace of the fabric tensor, i.e. the number of contacts of a particle. Furthermore, Young's modulus and the shear modulus are plotted, respectively, as a function of this coordination number in the Fig 5 B and 5 C.The behaviour also is roughly linear for both cases. A similar plot for Poisson's ratio as a function of the fabric is plotted in Fig. 5D. In this case, the behaviour is nonlinear, but a simple linear relationship is not expected, obviously.

6. Dstribution of stress and strain invariants

We plot in the Fig.6 the trace of the (negative) incremental stress tensor as a function of the trace of the (negative) strain tensor. The graph shows that the behaviour is nonlinear. The flat part of the graph corresponds to the points that are close to the surface of the sand pile. The slope of this graph is the differential bulk modulus; we observe that it decreases smoothly near the surface and there is a smooth transition from elastic to plastic behaviour rather than a discontinuous one. What is interesting about this graph is that we have (roughly) linear elastic behaviour for large strains and stresses and nonlinear behaviour announcing the transition to plastic behaviour for smaller strains, contrary to what one sees in solid state mechanics, where the plastic behaviour is a consequence of large loads. Of course, this is due to the noncohesive nature of the granular medium. Under compressive external load the pile behaves mostly elastic, but when this load becomes small or negligible, the lack of attractive interaction between the particles makes itself felt, the sand starts act like an isostatic network, which is almost flexible, and hence plastic.

Similar behaviour was observed in the analytical approach [1] for sand piles obtained by Didwania, Cantelaube, and Goddard as they assumed linear elastic behaviour near the centre and plastic behaviour closer to the surface of the sand pile.

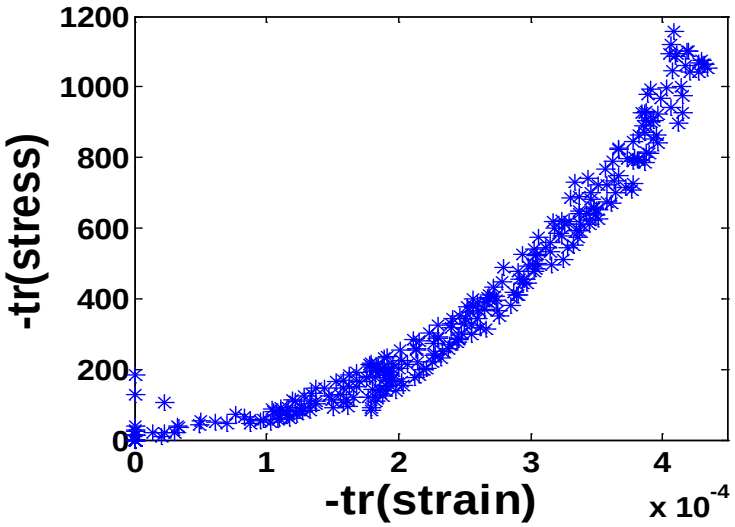

Fig.6 Correlation between trace of the incremental stress tensor and trace of the strain tensor.

7 Conclusions

To conclude, we have performed simulations of two-dimensional granular aggregates consisting of convex polygons and measured microscopic force distributions of the resulting "sand piles". Via averaging over representative volume elements, for which a sufficient size was determined to contain 100-200 particles, we have determined stress, strain and fabric distributions. To obtain a measure for strain, the sand pile was allowed to relax under reduction of gravity. While it may be difficult or impossible to determine the strain tensor in an experimental sand pile, it is feasible to obtain an order-of-magnitude estimate for it from simu-

lations. We define the strain with respect to a hypothetical reference state of zero gravity. This reference state may be approximated from the static pile obtained in a simulation by slowly changing gravity and following the particle trajectories during the ensuing load change. Then, it is easy to compute the macroscopic strain tensor by averaging over an RVE. It turns out that the size of the RVE we need for converged strain tensors is the same as for stress tensors. For total strains, the procedure gives an estimate, which is best for the u_{yy} component, for incremental strains, it allows their precise measurement.

We find that the vertical normal strain u_{yy} is not only minimum at the bottom layer, but also in higher layers of the sand piles constructed from a point source. However, it disappears in layers near the tip of the pile. A similar vertical normal strain minimum was not obtained in piles poured from a line source, which demonstrates that the construction history affects the strain distribution under a sand pile.

In the next step, we determined the elastic constants assuming Hooke's law throughout the sand piles that are poured from a point source and the correlation between the elastic material constants and the fabric tensor. We observed that the bulk modulus of the sand pile, i.e. the stiffness of the granulate is a linear function of the trace of the fabric. Then we determine the correlation between invariants of the stress and strain tensor for a change in gravity of about 15%; the observed stress and strain relation is nonlinear. While we have linear elastic behavior near the centre of the pile, there is nonlinear behavior announcing the transition to plastic behavior near the surface of the sand piles as the same behavior was assumed by Cantelaube et al. [1]. We observe that the macroscopic tensors stress and fabric are not collinear in the sand pile.

References

[1] Didwania, A. K. , Cantelaube, F., Goddard, J. D.: Static multiplicity of stress states in granular heaps. Proc. R. Soc. Lond. A **456**, 2569-2588, (2000).

[2] Wittmer, J. P. , Cates, M. E., Claudin, P.: Stress propagation and Arching in Static Sand piles. J. Phys. I France **7**, 39 -80 (1997).

[3] Vanel, L., Howell, D., Clark, D., Behringer, R.P., Clement, E., Phys. Rev. E 60, R5040 (1999).

[4] I.Zuriguel, T.Mullin, and J.M. Rotter, Physical Review Letters 98,028001 (2007).

[5] Gear.C.W.: Numerical Initial Value Problems in Ordinary Differential Equations. Prentice-Hall (1971).

[6] Schinner, A.: Ein Simulationssystem für granulare Aufschüttungen aus Teilchen variabler Form. PhD thesis, Univ. Magdeburg (2001).

[7] Cundall, P. A., Strack, O. D. L.: A discrete numerical model for granular assemblies. Géotechnique **29**, 47 -65 (1979).

[8] K. Bagi. Stress and strain in granular assemblies. Mechanics of materials, 22:165-177, (1996).

[9] M. Satake. Three-dimensional discrete mechanics of granular materials. In N.A. Fleck and A.C.E. Cocks, editors, IUTAM symposium on mechanics of granular and porus Materials, Pages 193-202, Kluwer Academic Publishers, 1997.

[10] Cambou,B., Chaze, M., Dedecker, F., 2000. Change of scale in granular materials. Eur.J.Mech. A/Solids 19, 999-1014.

[11] J.D. Goddard, continuum modeling of granular assemblies. Physics of Dry Granular media. Eds.: H,J. Herrmann, J.p. Hovi and S. Luding, Kluwer Academic Publishers,Dordrecht, (1998),p.1-24

[12] S.C.Cowin, A simple theory of instantaneously induced anisotropy.Micromecanics of granular Materials. Eds.: J.T. Jenkins and M.Satake, Elsevier, Amsterdam, (1988), P.71.80.